Journal of Biomedical Science (2007) 14:699–716
DOI 10.1007/s11373-007-9182-2

The vicissitudes of the pacemaker current I_{Kdd} of cardiac purkinje fibers

Mario Vassalle
Department of Physiology and Pharmacology, Box 31 State University of New York, Downstate Medical Center, 450 Clarkson Avenue, Brooklyn, NY, 11203, USA

Received 6 March 2007; accepted 10 May 2007

Key words: potassium current I_{Kdd} underlying diastolic depolarization, hyperpolarization-activated current I_h (or I_f), cardiac Purkinje single cells, sino-atrial node, cesium, barium, K^+ depletion

Summary

The mechanisms underlying the pacemaker current in cardiac tissues is not agreed upon. The pacemaker potential in Purkinje fibers has been attributed to the decay of the potassium current I_{Kdd}. An alternative proposal is that the hyperpolarization-activated current I_f underlies the pacemaker potential in all cardiac pacemakers. The aim of this review is to retrace the experimental development related to the pacemaker mechanism in Purkinje fibers with reference to findings about the pacemaker mechanism in the SAN as warranted. Experimental data and their interpretation are critically reviewed. Major findings were attributed to K^+ depletion in narrow extracellular spaces which would result in a time dependent decay of the inward rectifier current I_{K1}. In turn, this decay would be responsible for a "fake" reversal of the pacemaker current. In order to avoid such a postulated depletion, Ba^{2+} was used to block the decay of I_{K1}. In the presence of Ba^{2+} the time-dependent current no longer reversed and instead increased with time and more so at potentials as negative as −120 mV. In this regard, the distinct possibility needs to be considered that Ba^{2+} had blocked I_{Kdd} (and not only I_{K1}). That indeed this was the case was demonstrated by studying single Purkinje cells in the absence and in the presence of Ba^{2+}. In the absence of Ba^{2+}, I_{Kdd} was present in the pacemaker potential range and reversed at E_K. In the presence of Ba^{2+}, I_{Kdd} was blocked and I_f appeared at potentials negative to the pacemaker range. The pacemaker potential behaves in a manner consistent with the underlying I_{Kdd} but not with I_f. The fact that I_f is activated on hyperpolarization at potential negative to the pacemaker range makes it suitable as a safety factor to prevent the inhibitory action of more negative potentials on pacemaker discharge. It is concluded that the large body of evidence reviewed proves the pacemaker role of I_{Kdd} (but not of I_f) in Purkinje fibers.

Introduction

The pacemaker current underlying diastolic depolarization (DD) in Purkinje fibers has been attributed to either to the decay of the potassium current I_{Kdd} (the potassium current underlying DD [1, 2], the former I_{K2}) or to the activation of I_f (hyperpolarization-activated Na^+-K^+current [3, 4]). This disagreement is reflected in the different interpretations offered by several reviews [5–12].

The aim of the present review is to re-assess the whole problem of the pacemaker current in Purkinje fibers in the light of *available evidence for and against* a given interpretation. The retracing of the development of findings and conclusions concerning the pacemaker current in Purkinje fibers allows to critically analyze their validity.

*To whom correspondence should be addressed. Fax: +1-718-2703103; E-mail: mario.vassalle@downstate.edu

I_{Kdd} hypothesis of Purkinje fiber pacemaker current

Membrane potential recordings

Voltage- and time-dependence of slope conductance
The slope conductance decreases during DD [13], consistent with a decay of a K^+ conductance. However, I_{K1} decreases at voltages positive to the maximum diastolic potential (MDP), due to inward rectification [14, 15]. Therefore, the slope conductance could decrease mainly because DD (however induced) *could cause* a voltage-dependent decrease in conductance. Yet, if DD were due to the activation of I_f, the decrease in I_{K1} conductance would have to be large enough to reverse the increase in conductance associated with the activation of the I_f channel.

K^+-dependence of slope conductance
In quiescent sheep Purkinje fibers, decreasing $[K^+]_o$ from 5.4 to 2.7 mM does not increase the resting potential (Figure 1A), although the outward driving force for K^+ increases. The membrane resistance almost doubles in lower $[K^+]_o$ at a similar resting potential (Figure 1A), suggesting that failure of the resting potential to become more negative in lower $[K^+]_o$ is a decreased K^+ conductance, and not an increased Na^+ conductance [16, 17].

Phase 3 repolarization of driven action potentials (AP) attains a progressively more negative MDP as $[K^+]_o$ is reduced (Figure 1B). The undershoot (the difference between MDP and resting potential) is about 7 mV in 5.4 mM $[K^+]_o$ and about 17 mV in 2.7 mM $[K^+]_o$ [16], apparently because the AP causes a transient increase in a net outward current. Amplitude and slope of DD are greater in lower $[K^+]_o$ (Figure 1B, where the arrow points to the attainment of a similar end-diastolic potential in different $[K^+]_o$).

I_f deactivates on depolarization [3, 4], but to account for the larger undershoot in lower $[K^+]_o$, I_f would have to increase. Instead, in lower $[K^+]_o$ I_f decreases [3]. Also, the decrease in resting membrane conductance [16, 17] is not consistent with an increase in I_f (or in background Na^+ current). In this connection, hyperpolarizing current steps decrease DD slope (Figure 1F) and may induce quiescence [18], consistent with a decrease in I_{Kdd} (the potential being closer to E_K), but not with I_f activation (which increases at more negative potentials).

Voltage clamp studies in Purkinje strands

The pacemaker current was studied in short thin segments of Purkinje fibers using the two microelectrode voltage-clamp technique [1]. Clamping the membrane potential at MDP in spontaneously active Purkinje fibers, caused an increasing net inward current, which accounted for the DD seen after the previous AP (Figure 1C). During voltage-clamp at the MDP in 5.4 (driven) and 2.7 mM $[K^+]_o$ (spontaneous), in the lower $[K^+]_o$ the inward current was larger and faster (Figure 1D). Accordingly, after the steps, the AP was followed by a larger and faster DD in the lower $[K^+]_o$ (arrows).

In Figure 1E, steps applied in 5.4 and 2.7 mM $[K^+]_o$ *from the resting potential* to the same hyperpolarized value resulted in a smaller instantaneous inward current jump in the lower $[K^+]_o$ (decrease in I_{K1}). After the jump, the time-dependent increase in net inward current indicated that the pacemaker current was partially activated at the resting potential. The pacemaker current was larger and faster in the lower $[K^+]_o$, consistent with the larger and faster DD that followed the step (arrows). These findings rule out that the decay of the delayed rectifier current I_K is responsible for DD, since the resting potential is negative to the threshold for I_K.

With the membrane clamped *at the maximum diastolic potential* (no role for voltage-dependent decrease in I_{K1}), the slope conductance decreased as a function of time during the clamp, indicating that the current was net inward because of a *time-dependent decrease in a K^+ conductance.* Indeed, the pacemaker current reversed at potentials negative to the potassium equilibrium potential (E_K): in 5.4 mM $[K^+]_o$, the reversal potential for I_{Kdd} was -86.4 ± 1.5 mV, not far from the calculated equilibrium potential (−89 mV) [1].

Noble and Tsien [19] found that the activation range of the K^+ pacemaker current (that they labeled I_{K2}) was between −90 and −60 mV, consistent with I_{Kdd} being present in the absence of AP (see Figure 1E, [1]). The current quickly activated on depolarization and underwent inward rectification [19]. The reversal potential

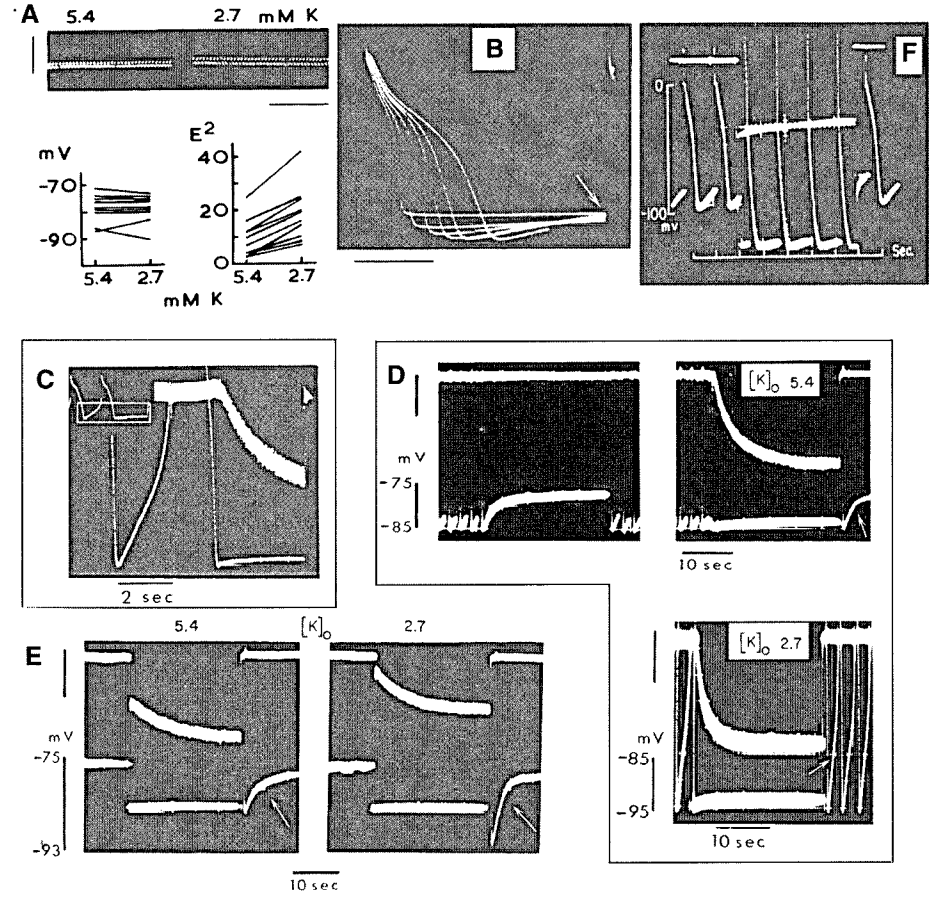

Figure 1. Voltage and current recording in Purkinje fibers superfused in Tyrode solution. *Panel A.* The slope conductance was measured in 5.4 and 2.7 mM $[K^+]_o$ in quiescent Purkinje fiber by superimposing hyperpolarzing pulses on the resting potential. The graphs underneath show that in the lower $[K^+]_o$ the resting potential changed little whereas the resting slope conductance consistently increased. *Panel B.* Action potentials recorded while decreasing $[K^+]_o$ from 5.4 (shortest action potential) to 1.8 mM (gradually longer action potentials). (Reproduced from Ref. [16] with permission of the American Physiological Society). *Panel C.* Recording of pacemaker current in a spontaneously active Purkinje fiber. The thin traces are the voltage records and the thick trace the current record. The current became increasingly inward as a function of time when the voltage was clamped at the maximum diastolic potential of the second action potential *Panel D.* Pacemaker current in 5.4 and 2.7 mM $[K^+]_o$. The top trace shows the current record in the absence of voltage clamping (first top D panel) as well as in the presence of voltage clamping at the maximum diastolic potential in 5.4 mM $[K^+]_o$ (second top D panel), and in 2.7 mM $[K^+]_o$ (bottom D panel) *Panel E.* Pacemaker current (thicker trace) during the same size hyperpolarizing steps from the resting potential in 5.4 and 2.7 mM $[K^+]_o$. (Reproduced from Ref. [1] with permission of the American Physiological Society). *Panel F.* Hyperpolarization decreases the pacemaker potential (reproduced from Ref. [18] with permission of the Rockefeller University Press, © 1961).

shifted 60 mV per tenfold change in $[K^+]_o$ [19–21], suggesting a specific K^+ current.

The time-dependent decrease in diastolic conductance, K^+-dependence, similar changes in size and slope of I_{Kdd} and of DD in different $[K^+]_o$, reversal of I_{Kdd} at E_K, 60 mV shift of reversal potential with a 10-fold change in $[K^+]_o$ led to the accepted conclusion that Purkinje pacemaker current was the specific K^+ current I_{Kdd}.

Limitations of approaches used for the study of I_{Kdd}

Discovery of I_f in the SA node and similarities with I_{Kdd}

In the sino-atrial node (SAN), an inward current was discovered [22, 23] that activated on hyperpolarization, a finding soon confirmed [24–31]. The current (labeled I_h) activated slowly at

potentials negative to the dominant DD range, and it would prevent the hyperpolarization of dominant pacemakers by electrotonic interaction with the more negative diastolic potential of atrial cells [29].

However, others proposed that I_h (which was labeled I_f [26, 27, 31]) was the pacemaker current in SAN and that it had properties very similar to those of I_{K2} in that both currents activated within a similar voltage range (−60 to −100 mV), contributed to the positive chronotropic effect of catecholamines [26, 28, 32], depended on $[Na^+]_o$ [27, 33], and were blocked by Cs^+ [27, 34, 35]. In spite of similarities, I_f did not behave like a pure K^+ current, depended on $[Na^+]_o$ and underwent an increase in conductance, consistent with an inward sodium-potassium current activated on hyperpolarization [27]. The similarities were taken to suggest that I_f and I_{K2} in Purkinje fibers might be the same current and the dissimilarities that I_{K2} might have been misinterpreted [3, 27].

K^+ depletion, "fake" reversal potential and use of barium

The occurrence of depletion of K^+ in narrow extracellular clefts (K_c) during hyperpolarizing steps negative to E_K [36, 37] seemed to receive support by the finding that the pacemaker current reversal potential was 5–15 mV negative to calculated E_K [19–21]. However, the current phase attributed to K_c depletion [36, 37] was not suppressed by Ba^{2+} (which prevents K_c depletion) [38]. In addition, in Purkinje strands, if the voltage during large hyperpolarizing clamp steps is not uniform, E_{rev} shifts in a negative direction with respect to E_K and more so with larger voltage non-uniformity (larger hyperpolarizations) [39].

Pretty soon, it was proposed that K_c depletion due to hyperpolarization would induce a time-dependent decrease in inward I_{K1} current which would cause a "fake" reversal [10]. Because of this possibility, a decrease in membrane conductance during the pacemaker current [1] and the shift of the reversal potential in different $[K^+]_o$ [19–21] (the conductance of I_{K1} channel being very sensitive to $[K^+]_o$) were no longer considered to provide support for I_{Kdd} hypothesis [3, 4, 10].

Na^+-dependence of the pacemaker current

A lower $[Na^+]_o$ decreases DD slope [16, 40] and the pacemaker current disappears in the pacemaker range in Na^+-free solution [33]. This was considered a rather peculiar behavior for a pure K^+ current (see [6]).

In conclusion, it was proposed that I_f was the pacemaker current in both SAN and Purkinje fibers and that the spurious effects of K_c depletion would mask I_f in the latter tissue. The previous findings were not disputed [6], only their interpretation. They were accounted for in a different way also by using computer modeling [41].

I_f hypothesis of Purkinje fiber pacemaker current

The following approaches were used to demonstrate that I_f was the "real" pacemaker current.

Specific block of I_f by Cs^+

In SAN, Cs^+ blocks I_f (e.g. [27, 35]). In Purkinje fibers in Tyrode solution, I_f is not apparent, but Cs^+ blocks the pacemaker potential [34, 42] and current [34]. Because Cs^+ abolished I_{K2} while shifting outwardly the total current (Figure 2A, left panel), it was proposed that Cs^+ *specifically* blocks the inward I_f [3].

Block of K^+ depletion in narrow clefts (K_c) by Ba^{2+}

Ba^{2+} blocks I_{K1} (and therefore K_c depletion) and in SAN has little or no effect on I_f [30]. In the presence of Ba^{2+} (5–10 mM), the time-dependent current did not reverse any longer on hyperpolarization to potentials negative to E_K (e.g., −111 mV in 9 mM Tyrode, Figure 2B), as expected for I_f. Also, membrane conductance increased during I_f (Figure 2C) [3]. I_f reversed at potentials positive to −50 mV and the reversal potential shifted in a negative direction in lower $[Na^+]_o$ and in a positive direction in higher $[K^+]_o$. The channel conductance was increased by higher $[K^+]_o$ [4]. In the presence of Ba^{2+}, Cs^+ blocked I_f which was assumed to be the same current that Cs^+ blocked in Tyrode solution.

All these findings were interpreted to mean that Ba^{2+} prevented the masking of I_f by K_c depletion,

that Cs^+ specifically blocked I_f and that I_f was a mixed Na^+ and K^+ pacemaker current.

Computer reconstruction

Computations showed that in Tyrode solution during hyperpolarizing steps K_c depletion would lead to g_{K1} decrease, progressive I_{K1} decrease, spurious reversal at E_K and masking of I_f. Also, the current reversal shift in different $[K^+]_o$ (expected for a K^+ pacemaker current) was attributed to the fact that K_c depletion was a function of g_{K1}, which increases with higher $[K^+]_o$ [41]. In Tyrode solution, in SAN I_f is visible, because I_{K1} is too small to produce a sufficiently large depletion current to mask I_f [41].

Na^+-dependence of the pacemaker current

As mentioned above, the Na^+-dependence of the pacemaker potential and current was viewed as supporting the I_f hypothesis.

I_f in Purkinje single cells in the absence and presence of Ba^{2+}

In Purkinje single cells [43], in the absence of restricted extracellular spaces and of Ba^{2+}, there was a secondary decrease in time-dependent current on hyperpolarizations negative to about −100 mV. Since this secondary decrease disappeared in the presence of Ba^{2+}, the decline was attributed [43] to the gradual inactivation of I_{K1} at potential negative to E_K [44].

The HCN "pacemaker" channels

Hyperpolarization-activated HCN channels generate a current that, like the native I_f, activates on hyperpolarizations negative to −50/−70 mV, is carried by both Na^+ and K^+, does not inactivate, is increased by cyclic nucleotides, and is blocked by Cs^+ but not by Ba^{2+} (see [45] and below).

Modulation by neuromediators

Catecholamines increase I_f [26, 28] by shifting I_f activation curve in a depolarizing direction; acetylcholine (even in low concentrations) has the opposite effect [46]. Since the pacemaker activity is under autonomic control, the neuromediator modulation of I_f (and of HCN channels [5]) has been taken to support the role of I_f as pacemaker current [47].

The general conclusion was that the I_{Kdd} hypothesis was "deeply incorrect" and that I_{K2} in actuality was I_f [3, 4, 6, 10].

Limitations of the approaches used for the proposed pacemaker role of I_f

Substantial objections undermine the purported role of I_f as the pacemaker current in Purkinje fibers.

Dissimilarities between SAN and Purkinje fibers

Dissimilarities in pacemaker mechanisms

The pacemaker current in SAN and in Purkinje fibers *can not* have the same potential range, since DD range in SAN dominant pacemakers (∼−50 mV to ∼ −40 mV) is positive to that in Purkinje fibers (−90 to −60 mV). The threshold for I_f activation is negative to the pacemaker range in SAN [8, 29] and in Purkinje fibers [2, 48].

In SAN, during a time comparable to that of dominant DD, I_K decays relatively rapidly (time constant 0.37 s on return to −40 mV [23]) with no initial lag. In contrast, I_f hardly changes at −50/−60 mV during the first 200 ms [8, 49] and it activates with a time constant of 2–4 s at −70 mV [29]. I_f activation has a similarly slow kinetics in Purkinje fibers in the presence of Ba^{2+} [2, 3]: yet, DD slope and discharge rate are much faster in SAN dominant pacemakers than in Purkinje fibers. In Figure 2B [3], in 3 mM $[K^+]_o$ (plus 5 mM Ba^{2+}) I_f does not change with time or does so with a marked delay in the pacemaker range of potentials (steps to −71, −81, −91 mV [3]) (for the slow onset of I_f see also [50]). In higher $[K^+]_o$ the activation of I_f becomes greater and faster [3] (see Figure 2B) whereas the pacemaker potential (e.g. [1, 51]) and deactivation of I_{Kdd} [2, 21] become smaller and slower.

Different behavior of SAN and Purkinje fibers in different conditions

In SAN, Cs^+ blocks I_f over its activation range [35, 52], but only slightly decreases SAN discharge [35, 53]. Even 20 mM Cs^+ fails to stop the SAN

[53] (Figure 3A) and, in high $[K^+]_o$, Cs^+ may *initiate* spontaneous discharge with APs having an undershoot followed by DD (Figure 3B) [53]. Also, Cs^+ affects little I_{Ca} [35] and I_K [35, 52] which would readily account for the continued discharge in the presence of Cs^+-block of I_f.

In Purkinje fibers, pacemaker activity can occur in the normal range and at a depolarized potential range [6, 42, 54] (Figure 3C). In the normal range, 2 mM Cs^+ stops spontaneous discharge [34, 42] and blocks I_{Kdd} [2, 55, 56]. In contrast, Cs^+ fails to block the depolarized level DD (Figure 3C, [42]), which is due to I_K decay (see [6]). This is consistent with Cs^+ not blocking I_K and discharge in SAN [35, 52].

Also, SAN continues to discharge in 10–15 mM $[K^+]_o$ [57–60] whereas Purkinje fibers become quiescent in $[K^+]_o$ above some 3 mM [61]. High $[K^+]_o$ has little direct effect on I_K [62] whereas it decreases Purkinje DD [61] and I_{Kdd} [1, 2, 21]. High $[K^+]_o$ increases I_f [3], but decreases SAN rate by modifying the oscillatory potentials [57].

Non-specificity of Cs^+ as a blocker of I_f

The rationale for the specificity of Cs^+-block of I_f

I_{Kdd} is partially activated at the resting potential [1, 2] and, on hyperpolarization, I_{K1} and I_{Kdd} decrease instantaneously (e.g., they disappear at E_K). Their decrease contributes to the instantaneous inward current jump. Cs^+ blocks I_{Kdd} at the holding potential (V_h) and, in the steady state, shifts the holding current in an inward direction, as expected from a block of an outward current [34, 55]. If already blocked by Cs^+ at V_h, on hyperpolarization I_{Kdd} would decrease less than in control and this smaller decrease would contribute less to the instantaneous inward current. Also, I_{Kdd}, being already blocked at V_h, would not

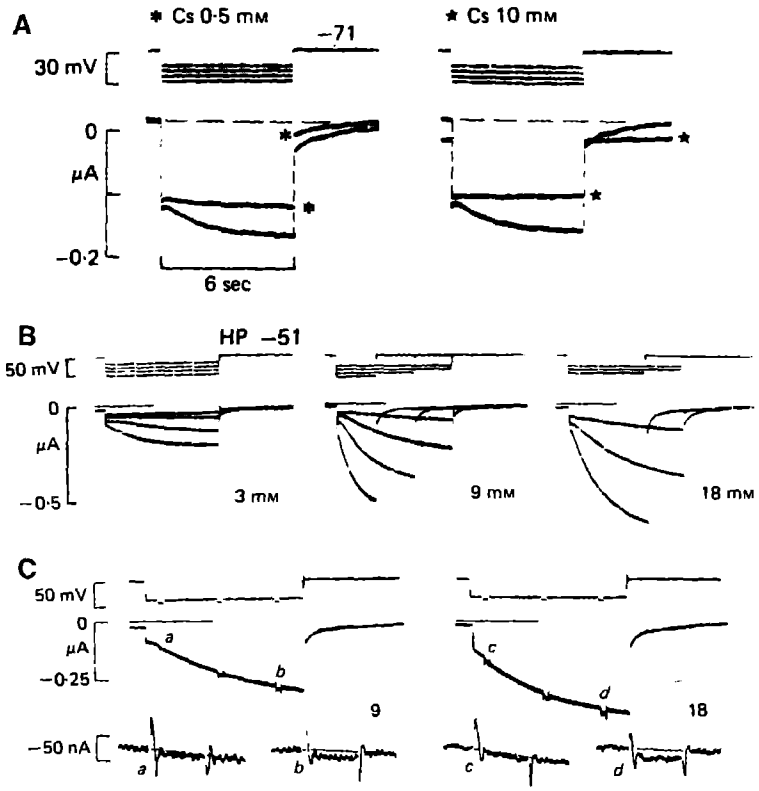

Figure 2. The hyperpolarization-activated current I_f in Purkinje fibers under different conditions. *Panel A.* Effects of Cs^+ in Tyrode solution. Hyperpolarizing steps were applied from −71 to −101 mV in the absence and presence (asterisks) of 0.5 and 10 mM Cs^+. *Panel B.* In the presence of 5 mM Ba^{2+}, I_f appeared during hyperpolarizations in 3 mM $[K^+]_o$ (from −51 to −121 mV) and increased in 9 mM $[K^+]_o$ (largest hyperpolarization −111 mV) and 18 mM $[K^+]_o$ (largest hyperpolarization −101 mV). *Panel C.* Increase in slope conductance during the activating I_f on hyperpolarization from −40 mV in 9 mM and 18 mM $[K^+]_o$. Bottom traces were recorded at higher speed. (The traces selected are reproduced from Ref. [3] with permission of the Physiological Society).

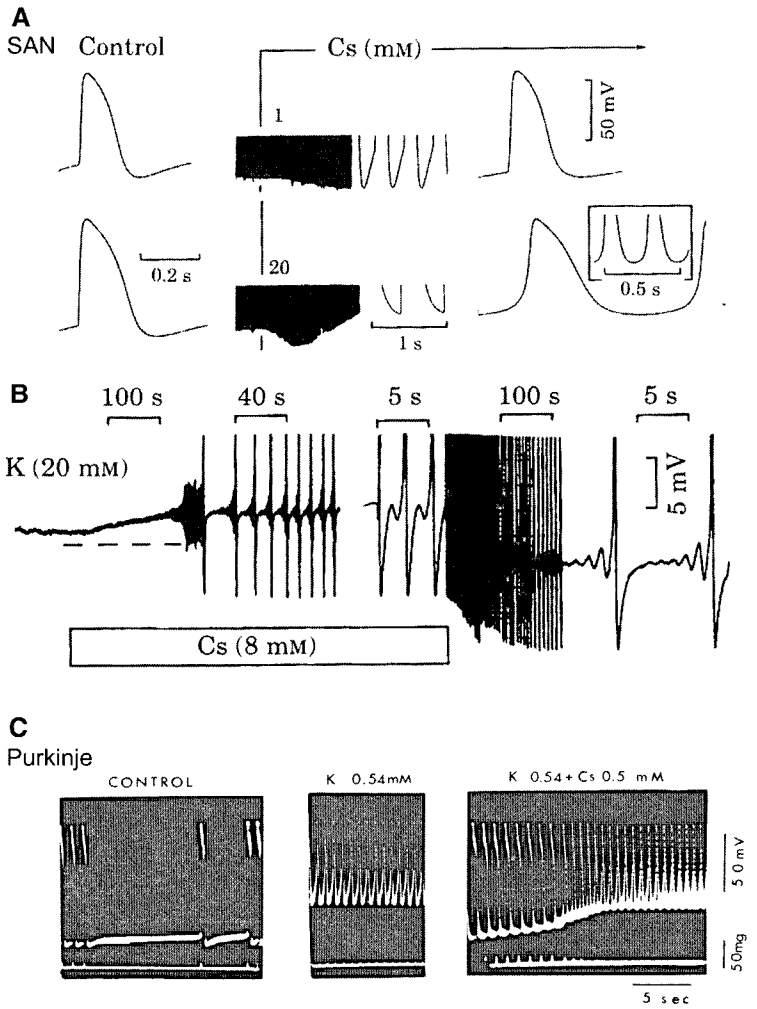

Figure 3. Cs^+ does not suppress the discharge of the sino-atrial node (SAN) nor that of Purkinje fibers at depolarized level in low $[K^+]_o$. *Panel A.* SAN discharge was not suppressed by 1 mM (top trace) or by 20 mM Cs^+ (bottom trace) in Tyrode solution. *Panel B.* The SAN was quiescent in 20 mM $[K^+]_o$. Cs^+ (8 mM) decreased the resting potential and induced increasing oscillatory potentials that led to spontaneous discharge. (Modified and reproduced from Ref. [53] with permission of Elsevier). *Panel C.* The first C panel shows Purkinje fiber action potentials at normal $[K^+]_o$ and the middle C panel the action potentials at depolarized level in low $[K^+]_o$. In the last C panel, low $[K^+]_o$ depolarized the membrane as before, but Cs^+ did not suppress the fast discharge at depolarized level (whereas it suppressed DD at the normal polarized level, not shown). (Reproduced from Ref. [42] with permission of the American Physiological Society).

change as a function of time during step. Therefore, the decrease in total current by Cs^+ during a hyperpolarizing step does not imply a specific block of I_f.

Block of other K^+ channels by Cs^+

Cs^+ blocks I_f in the SAN [e.g., 27, 35, 52] and, in the presence of Ba^{2+}, in Purkinje fibers [2, 3, 43] and ventricular myocytes [48, 63]. However, in ventricular myocytes, Cs^+ blocks also the pacemaker potential and current induced by the time- and voltage-dependent block of I_{K1} by Ba^{2+} [64, 65]. Although this pacemaker current (it may lead to spontaneous discharge) is different from I_{Kdd}, still Cs^+ blocks a current that is certainly a K^+ pacemaker current (and not I_f). Cs^+ also blocks different K^+ currents in different tissues (see [66] for references) and radioactive potassium fluxes in cardiac tissues [67]. Therefore, a block of a pacemaker current by Cs^+ does not provide unequivocal evidence that the blocked current is I_f.

Actions of Cs^+ that could be related to a block of I_f
In Purkinje fibers, Cs^+ increases the resting potential [66–69], and decreases intracellular sodium activity (a^i_{Na}) [66, 70, 71]. Both actions could result either from a Cs^+-induced block of I_f [70, 71] or a Cs^+-induced stimulation of the activity [68] of the electrogenic [71] Na^+-K^+ pump ("Na^+ pump"). However, if Cs^+ acted by blocking I_f, it should induce a persistent decrease in a^i_{Na} and a persistent hyperpolarization. Instead, in quiescent Purkinje fibers Cs^+ induces a maintained decrease in a^i_{Na} [66, 68, 71], but only a transient hyperpolarization [66–69], as expected from the stimulation of the Na^+ pump current [34, 71]. Also, Cs^+ hyperpolarizes in situations where I_f is absent (zero $[K^+]_o$ or in myocardium at the resting potential) or is not activated (fibers driven at fast rate with very short diastole) [66] or is deactivated (depolarized levels in low $[K^+]_o$) [51]. Accordingly, Cs^+ hyperpolarizes much less when the Na^+ pump is already stimulated by high $[K^+]_o$ (which increases I_f) or it is inhibited by strophanthidin [51, 66]. In conclusion, Cs^+ block of I_f is neither specific nor it is the only action of Cs^+.

Use of Ba^{2+} to block I_{K1} and the presumed K^+ depletion

The currents that might be blocked by Ba^{2+}
Ba^{2+} (a blocker of K^+ channels [3]) might have blocked the very current (I_{Kdd}) to be studied. A block of I_{Kdd} and the consequent abolition of its reversal might unmask I_f. Indeed, in 4 mM $[K^+]_o$, Ba^{2+} consistently *reduced* the pacemaker current at potentials positive to about −95 mV and *increased* it at more negative potentials. The difference current (the current eliminated by Ba^{2+}) reversed on hyperpolarization [38]. Decreasing $[K^+]_o$ from 4 to 2 mM shifted the reversal potential of the difference current to a more negative potential [38], as appropriate for a K^+-specific current. Also, low concentrations of Ba^{2+} that block I_{K1} (and therefore a possible K^+ depletion) may not affect the time-dependent current [38, 55].

K_c depletion in the DD range at potentials positive to E_K
In the DD range (positive to E_K), K^+ driving force is outward, raising the question as to whether a depletion in K_c can occur. Also, different concentrations of Ba^{2+} (0.05 to 5 mM) dissociate the changes in the initial inward current jump on hyperpolarization from those of the time-dependent current positive to −95 mV, suggesting that reduction of the pacemaker current was due to block by Ba^{2+} [38]. In Tyrode solution, experiments with Ba^{2+}, Cs^+, and high $[K^+]_o$ failed to detect K_c depletion in the pacemaker range [55]. Also, positive to E_K, I_{K1} undergoes a strong inward rectification [14, 15, 44, 72] and there is no I_{K1} inactivation as a function of time [44].

Another major point is that *at E_K, the net K^+ flux is zero and this would prevent any K^+ depletion.* In other words, *in Tyrode solution I_f should be present at least at E_K*: this does not occur, suggesting that I_f activates at more negative potentials.

K_c depletion at potentials negative to E_K and "fake" reversal of I_{Kdd}
As mentioned before, the initial inward decreasing current component on hyperpolarization attributed to K_c depletion [36] persists in the presence of 5 mM Ba^{2+} [38]. Also, the extracellular space is larger in dog Purkinje fibers and calculations suggested that depletion was not large enough to account for a pseudo-reversal near E_K [73]. Since I_f is not present in Tyrode solution in the absence of Ba^{2+}, whether Ba^{2+} unmasks I_f because it prevents K_c depletion or because it blocks I_{Kdd} can only be determined with Purkinje single cells, where there is no K_c depletion and can be studied in the absence and presence of Ba^{2+} (see below).

Computer reconstruction

The DiFrancesco-Noble computer model [41] had also some limitations. For example, the onset of I_f is sigmoid [50], but a first order kinetics for the gating parameter was assumed. To induce pacemaker activity, the y variable was shifted by 10 mV in a positive direction. The time constants of K_c depletion and of I_f gating were assumed to be of the same order of magnitude [6, 41], but the kinetics of I_f is significantly different from that due to a depletion-induced decrease in I_{K1} [74, 75].

The reversal of the diastolic time-dependent current negative to E_K was found both in Purkinje strands and in single Purkinje cells. It was considered spurious in both cases, although for different reasons: a decay of I_{K1} would occurs in the

Purkinje strands because of the depletion of K_c [5, 6] and in Purkinje cells because of a voltage- and time-dependent inactivation of I_{K1} [43].

A time-dependent inactivation of I_{K1} should have occurred at potentials negative to E_K also in the intact strands, in addition to the effects of K_c depletion. However, on the basis that the time-dependent inactivation of I_{K1} becomes important only at very negative potentials, time-dependent inactivation of I_{K1} was not used in computer model of DiFrancesco and Noble [41]. Therefore, for the computer model a finding was used (K_c depletion) that later was abandoned in favor of a time-dependent inactivation of I_{K1} at negative potentials. Yet, the latter was not used in the model computations due to its occurrence at potentials well negative to E_K. The model was considered primarily descriptive [41] and in fact the electrical activity of Purkinje fibers had been also reconstructed previously using I_{Kdd} as the pacemaker current [76].

Na^+-dependence of the pacemaker current

In Purkinje fibers a lower $[Na^+]_o$ reduces the slope of DD [16, 40], since, for same decay in I_{Kdd}, the background Na^+ current becomes smaller. I_{Kdd} should disappear in Na^+-free solution, but only at potential positive to E_K. In fact, in a Na^+-free solution, during steps negative to E_K the inward current decayed with time, as expected from a decrease in an inward K^+ movement as a result of a time-dependent decrease in K^+ conductance [1]. In SAN, I_f disappears in Na^+-free solution, but 9 mM $[K^+]_o$ makes I_f to reappear [77] as hyperpolarization to potentials negative to the lower E_K allows K^+ to enter the cell.

The characteristics of the HCN channels

The characteristics of these channels [12, 45, 78–90] will be briefly considered here and then the specific question as to whether they are pacemaker channels and they provide evidence supporting a pacemaker role of I_f will be addressed.

Two classes of similar channels have been identified: cyclic nucleotide-gated (CNG) channels and hyperpolarization-activated cyclic nucleotide-modulated (HCN) channels. CNG and HCN channels have a similar structure and behavior. However, the activation of CNG channels is largely voltage-independent. Instead, the HCN channels activation is voltage-dependent [45] and show properties similar to those of native I_f (e.g., 45, 89, 91–95).

The four HCN subunits (HCN1–HCN4) [45] are expressed *in different tissues* such as photoreceptors, dorsal root ganglia, cortex, cerebellum, basal ganglia, subcortical areas, heart [96–98]. In the heart, HCN channels are expressed in pacemakers [93, 95, 99–101] and in non-pacemakers myocardial tissues [99, 101, 102]. The HCN channels are involved in *several functions* [45, 95, 103–108], most of which are not related to pacemaker activity. In heart tissues, the *distribution* of four HCN isoforms is not uniform. In SAN cells, the most highly expressed HCN channel is HCN4 [95, 99, 100, 102, 109], followed by HCN2 [95, 99, 102]. HCN2 is distributed also in atrial myocytes [102]. HCN1 has been detected in SAN of rabbits and mice [95, 99, 100]. HCN1 and HCN4 transcripts are expressed in rat and rabbit Purkinje fibers, HCN4 expression being lower in Purkinje than in SAN, but higher than that in ventricles [99].

Thus, the HCN4 isoform with the slowest activation [84, 110] predominates in SAN, which has the fastest DD. And HCN4 is expressed with HCN2 also in the non-pacemaking atrial tissues [102]. In rabbit SAN, HCN1 would play "a central and specific role in the formation of SAN pacemaker currents" [100], since it has the fastest kinetics. However, sensitivity to cAMP is poor for HCN1, high for HCN2 and highest for HCN4 channels [84, 111, 112]. The substantial response of native I_f to cAMP [113–115] is an indication that HCN4 is likely to represent a major component of I_f [99]. Also, HCN1 is prevalent [99] in Purkinje fibers which have a less steep DD. In the mouse SAN, HCN4 transcripts prevails [95] and yet the rate is of the order of 600/min [84] (cycles lasting 100 msec). In dog Purkinje fibers, HCN4 is the predominant isoform as in SAN [101] and yet their discharge is far slower.

Different HCN isoforms are also expressed in atrial and ventricular myocytes where I_f has been also reported [48, 63, 95, 99, 101, 116–118]. Therefore, there is no correlation between expression of HCN channels in different tissues and pacemaker activity.

As for the *kinetics*, HCN currents have a sigmoid onset and a slow activation, as I_f does.

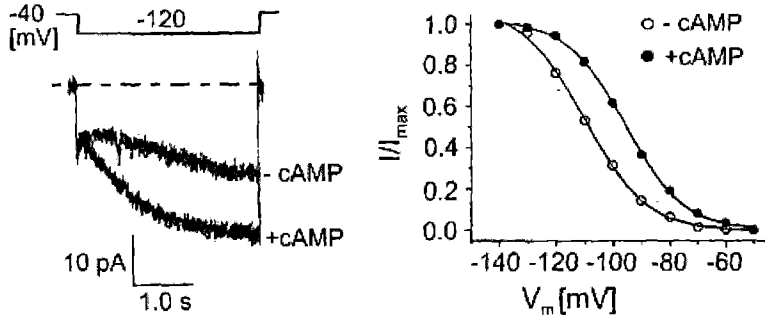

Figure 4. Modulation of the current of the hyperpolerization-activated cyclic nucleotide-gated (HCN4) channel by cyclic adenosine monophosphate (cAMP). *Panel A.* HCN4 was expressed in HEK293 cells. Current traces were measured in an inside-out patch at −120 mV in the absence of cAMP (−cAMP), and in the presence of a saturating (10 mM) concentration of cAMP (+cAMP). *Panel B.* Activation curves of HCN4 currents measured in whole-cell clamp mode in the absence (−) or presence (+) of 1 mM of cAMP. (Reproduced from Ref. [84] with permission from Elsevier).

The time constant of activation of HCN4 is very slow at −70 mV [84, 93, 94, 110]. In Figure 4A [84], a hyperpolarizing step to −120 mV still involved a long delay in HCN4 current activation: during initial 0.5 s (longer than DD) the inward current was actually *de*creasing (e.g., see also Figure 4F in [110]; or Figure 3, −75 and −85 mV traces in [119]). The time constant of current activation is often measured after excluding the initial lag in current activation [e.g., 19, 95, 112]. Yet, the initial lag phase is incompatible with DD.

As for *the activation range*, HCN channel currents start activating at potentials negative to −60 mV [91–93, 95, 109] over a range negative to that of dominant APs, as I_f does. For example, in Figure 4B, the HCN4 current started activating at potentials negative to −70 mV [84]. While there are differences in different reports about activation range and kinetics of different HCN currents, still (like for I_f) HCN activation curve has been overwhelmingly found negative to the dominant DD range.

Native I_f and I_f channel currents are measured during steps lasting several seconds. With steps to −60 and −70 mV there might be no activation at all over a period of time similar to that of DD (i.e., ~200 ms): if currents were measured at that short interval, the activation curve would shift to even more negative potentials [94, 97]. The overexpression of the HCN2 subunit increases the amplitude of that current, but even so it has no effect on activation range [120].

Modulation by cAMP. As with I_f [113, 114], cAMP shifts HCN channel activation in a depolarized direction, speeds activation kinetics, and increases the maximal current at hyperpolarized voltages [45, 92, 121–123] (see Figure 4A). Administration of cAMP shift the half maximal activation voltage ($V_{1/2}$) of HCN1 channels by 2–5 mV and that of HCN4 channels by approximately 15 mV [109]. However, $V_{1/2}$ is far more negative than the threshold for I_f activation. In Figure 4B, cAMP shifted $V_{1/2}$ of HCN4 by 15 mV in a positive direction, but had little effect at −50 and −60 mV, as shown also by others (see Figure 4 in [91]; Figure 4 in [110]; Figure 4 in [118] or Figure 4 in [121]). SAN dominant APs do not physiologically attain $V_{1/2}$. These features are seen in different reports with a degree of variation related to different factors, including the protocol adopted [109] or the HCN isoform (see Figure 10 for HCN2 in [122]). In any case, SAN rate is fast also in vitro (no tonic or phasic sympathetic nerve regulation). The direct regulation by cAMP is present also in non-pacemaking ventricular myocytes [118] and in CNG channels (45).

Because HCN channel currents have drawbacks similar to those of native I_f (as one would expect), they fail to provide support for a cardiac pacemaking role of I_f, Similar considerations apply to also to Purkinje fibers, where I_f activation curve is also shifted to values negative to the pacemaker range [2, 48].

Specificity of bradycardic agents. In actuality, these agents are not specific since they also block currents other than I_f [124–126]. Clinical concentrations of UI-FS 49 decreased I_{Ca} (thereby slowing the SAN) while having little effect on I_f [125]. ZD7288 inhibited I_f at −120 mV, but there was no I_f at −50 and −60 mV both in control and in the

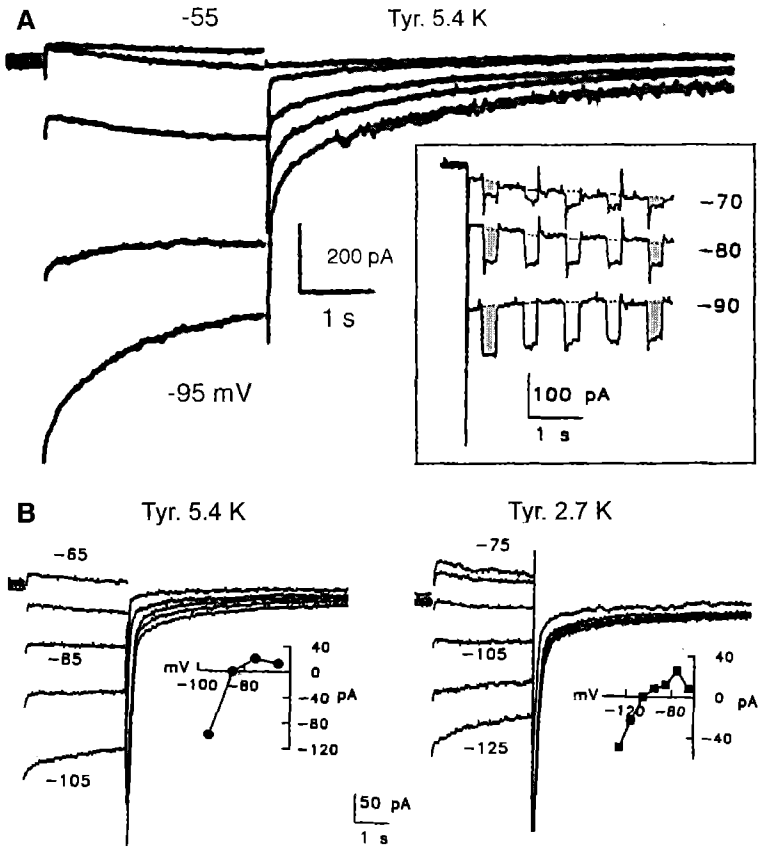

Figure 5. The reversal of the pacemaker current I_{Kdd} and its dependence on $[K^+]_o$ in Purkinje single cells. *Panel A.* The current records during hyperpolarizing steps varying from −55 to 95 mV in increments of 10 mV show the reversal of I_{Kdd}. The boxed inset shows the decrease in slope conductance (measured by the amplitude of the superimposed pulse currents, cf. gray areas) during I_{Kdd} at potentials above and below E_{rev}. *Panel B.* Shift of E_{rev} of I_{Kdd} from −85 mV in 5.4 mM $[K^+]_o$ to −105 mV in 2.7 mM $[K^+]_o$. (Modified and reproduced from Ref. [2] with permission of The Rockefeller University Press, © 1961).

presence of the drug. ZD7288 decreased also I_K by 33% and I_{Ca} by 15% [124]. Zatebradine blocks the delayed rectifier I_K [126] and in CNS, ZD7288 blocks responses that are unrelated to I_f [127]. Ivabradine has been studied in the presence of Ba^{2+} and Mn^{2+} with steps to −100 mV [128]. Under those conditions, changes of I_{Ca} and I_K that might affect SAN rate would not be seen, since these currents were already blocked and no depolarizing steps were applied. In conclusion, the bradycardic agents inhibit I_f at potentials negative to the dominant pacemaker range, but such an inhibition is not specific and can not be taken to underlie the much smaller decrease in SAN discharge.

SAN dysfunction can be induced by *knockout of I_f channels* [129]. However, dysfunction of SAN discharge is induced also by knockout of Na^+ channels [130] and of Ca^{2+} channels [131–133].

In conclusion, in cardiac tissues HCN channels generate currents whose characteristics are quite suited for a hyperpolarization-activated current (I_h), but not for a pacemaker current.

Action of neuromediators

Catecholamines increase I_{Ca} and modulate I_f also in myocardial cells (no pacemaking) [134, 135]. In SAN, catecholamines increase not only I_f [26], but also I_{Ca} and I_K [26, 28, 35] which are important for discharge [6]. Cs^+ block I_f (but not I_K and I_{Ca}): yet, adrenaline increases rate and I_{Ca} *during the persisting Cs^+ block of I_f* [35]. In 15 mM Cs^+, norepinephrine increases SAN rate of discharge as it does in control [136].

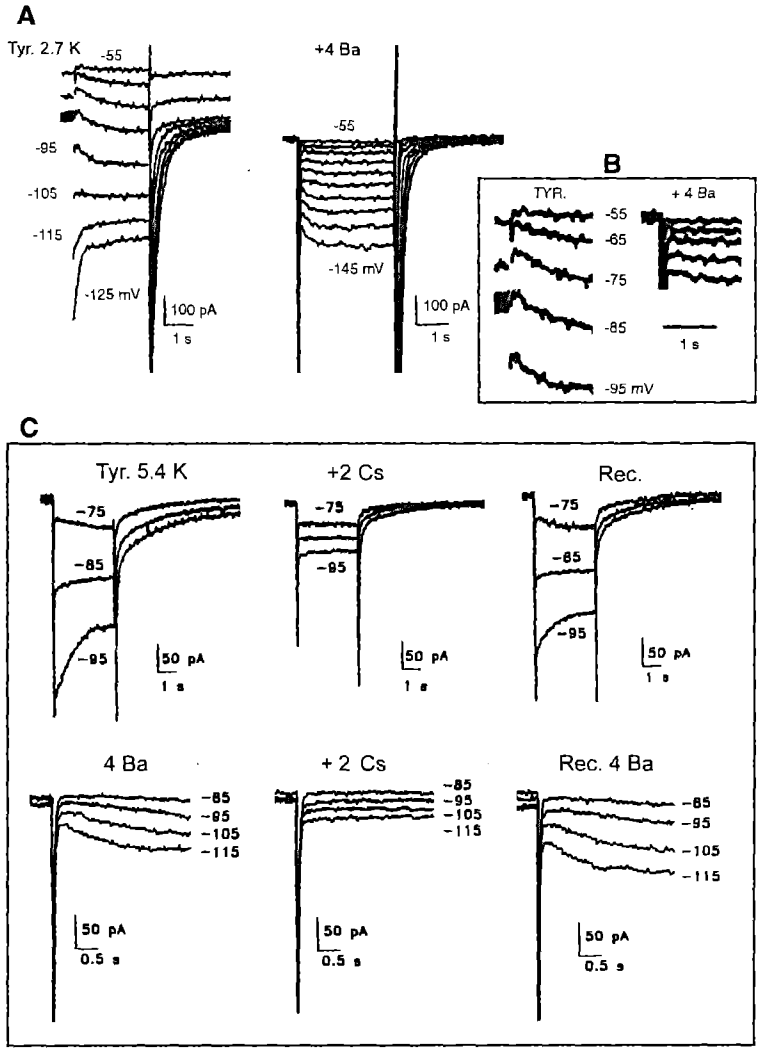

Figure 6. Barium suppresses the pacemaker current I_{Kdd} and unmasks the hyperpolarization-activated I_f whereas Cs^+ suppresses both currents. *Panel A.* The first A panel shows the deactivation of I_{Kdd} during hyperpolarizing steps varying from −55 to −125 mV in increments of 10 mV. The second A panel shows the current traces during the same protocol in the presence of 4 mM Ba^{2+} (suppression of I_{Kdd} and unmasking of I_f). *The boxed inset B* compares the large I_{Kdd} (deactivating without a delay) and the smaller I_f (slowly activating at more negative values). *Panel C.* In Tyode solution (upper C panels) 2 mM Cs^+ suppresses I_{Kdd} and in the presence of 4 mM Ba^{2+} (lower C panels) 2 mM Cs^+ suppresses I_f. The effects of Cs^+ were reversible. (Modified and reproduced from Ref. [2] with permission of The Rockefeller University Press, © 1961).

The unraveling of the contradictions about the pacemaker current

The separation of the pacemaker current I_{Kdd} from the hyperpolarization-activated I_h

To verify the major assumptions about the purported pacemaker role of I_f, the pacemaker current was investigated by means of whole cell patch clamp method in Purkinje single cells in the absence of K_c depletion and of Ba^{2+} as well as in the presence of Ba^{2+} and/or Cs^+ [2].

In Tyrode solution, hyperpolarizing steps from V_h of −50 mV resulted in a time-dependent current with a threshold of about −60 mV and reversal near E_K (I_{Kdd}) (Figure 5A). The slope conductance decreased during I_{Kdd} (cf. gray areas in boxed inset). In Figure 5B, decreasing $[K^+]_o$ from 5.4 to 2.7 mM shifted the reversal potential of I_{Kdd} near the more negative E_K value. E_{rev} shifted from

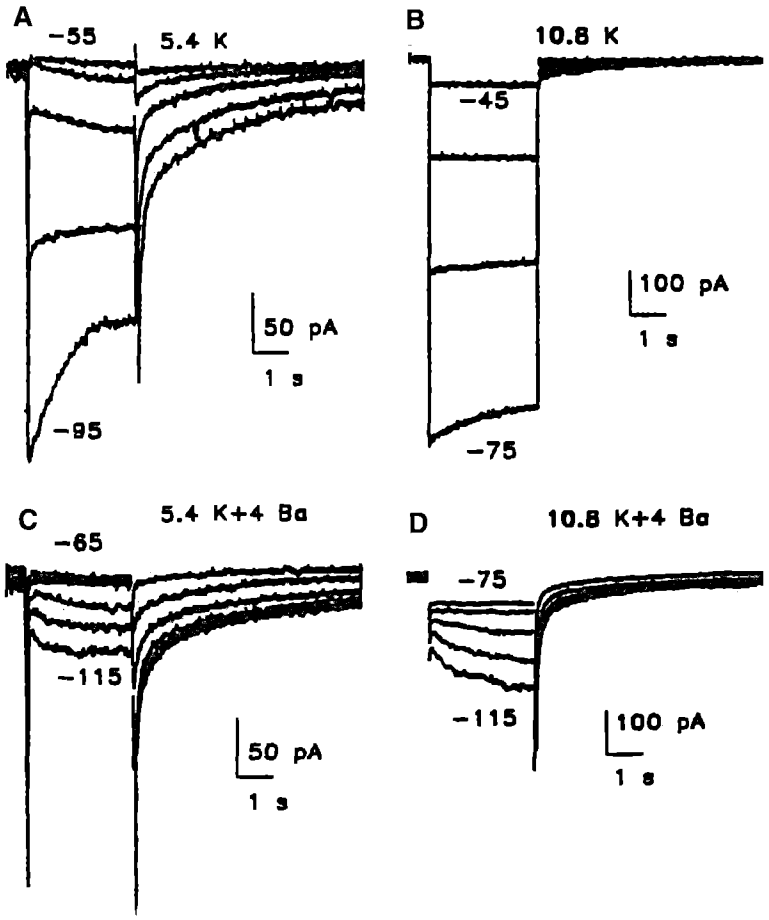

Figure 7. High $[K^+]_o$ decreases I_{Kdd} in Tyrode solution and increases the hyperpolarization-activated I_f in the presence of Ba^{2+}. *Panel A.* I_{Kdd} was recorded in 5.4 mM $[K^+]_o$ during hyperpolarizing steps varying from −55 to −95 mV in increments of 10 mV. *Panel B.* A similar procedure (steps varying from −45 to −75 mV) was repeated in 10.8 mM $[K^+]_o$, which markedly reduced I_{Kdd}. *Panel C.* Hyperpolarizing steps varying from −65 to −115 were applied in 5.4 mM in the presence of 4 mM Ba^{2+}, showing that I_f activated slowly at more negative potentials. *Panel D.* A similar procedure applied in 10.8 mM $[K^+]_o$ in the presence of 4 mM Ba^{2+} shows that (on contrast to I_{Kdd}) I_f became larger (note different calibration). As usual, I_f appeared at more negative potentials than I_{Kdd}. (Modified and reproduced from Ref. [2] with permission of The Rockefeller University Press, © 1961).

average values of −86 mV in 5.4 mM $[K^+]_o$ to −104 mV in 2.7 mM $[K^+]_o$, as the predicted E_K shifted from −87 to −106 mV.

In Figure 6A, in 2.7 mM K Tyrode solution, the reversal potential of I_{Kdd} was −105 mV. Adding 4 mM Ba^{2+} eliminated I_{Kdd} and unmasked I_f with a threshold of about −90 mV. This shows that *Ba^{2+} blocks not only I_{K1}, but also the pacemaker current I_{Kdd}*. During more negative steps, I_f increased in size and did not reverse. The boxed inset B shows that, with respect to I_{Kdd}, I_f was smaller, activated very slowly and at more negative potentials. In Figure 6C, 2 mM Cs^+ reversibly blocked both I_{Kdd} in Tyrode solution and I_f in the presence of 4 mM Ba^{2+}, demonstrating that Cs^+ is not a specific blocker of I_f.

In Figure 7A, I_{Kdd} reversed as usual and in Figure 7B, when $[K^+]_o$ was doubled to 10.8 mM, the initial current jump increased (greater I_{K1}), but I_{Kdd} decreased. In Figure 7C, Ba^{2+} blocked I_{Kdd} whereas I_f slowly activated at −95 mV. In Figure 7D, in 10.8 mM K Tyrode, I_{Kdd} was blocked by Ba^{2+} and a larger I_f began activating at −95 mV. With respect to Tyrode solution, in high $[K^+]_o$ I_{Kdd} became smaller whereas I_f became bigger (note the different voltage calibrations). The slope conductance decreased during I_{Kdd} in the DD range in Tyrode solution and increased during

I_f at potentials negative to the DD range in the presence of Ba^{2+} (see Figure 8 in [2]).

The results in single cells (no depletion in narrow extracellular clefts) demonstrate that I_{Kdd} (1) is present in the DD range, (2) undergoes a decrease in conductance, (3) has a faster kinetics than I_f (4) reverses at E_K, (5) decreases in higher $[K^+]_o$, (6) reverses at different potentials as a function of $[K^+]_o$ and (7) is blocked by Cs^+ at potentials positive and negative to its reversal. The approach also permitted to identify the effects of Ba^{2+}, namely, (8) *Ba^{2+} blocks I_{Kdd}* (and therefore its reversal disappears), (9) the block of I_{Kdd} by Ba^{2+} unmasks I_f at potentials negative to the DD range, (10) I_f has a much slower kinetics than I_{Kdd}, (11) magnitude and rate of activation of I_f increase during stronger hyperpolarization or in higher $[K^+]_o$, (12) slope conductance increases during I_f activation and (13) I_f is blocked by Cs^+ (as is I_{Kdd}).

These findings show the irrelevance of K_c depletion in determining the experimental results and those of the computer reconstruction. Indeed, there seems to be very little depletion: reversal potential for I_{Kdd} was -86.4 ± 1.53 in intact strands [1] and -86 mV in single cells [2]). When the reversal potential was found more negative than E_K in Purkinje strands [19–21], the non-uniformity of the voltage during the hyperpolarizing steps [39] might have been the major contributing factor. The above results show that *in Purkinje cells the pacemaker current is due to a time-dependent decrease in K^+ conductance in the pacemaker range*, as initially proposed [1], and that I_{Kdd} can be separated from the hyperpolarization-activated I_h.

Conclusions

The disagreement about the Purkinje fiber pacemaker current apparently resulted from the assumptions that (1) K_c depletion was large enough not only to mask the activating I_f, but also to induce a spurious reversal, (2) Ba^{2+} blocked I_{K1} (and therefore K_c depletion) but not I_{Kdd} (this question was not considered), (3) Cs^+ was a specific blocker of I_f and (4) the computer reconstruction provided support for the assumptions made.

The discovery of I_f in the presence of Ba^{2+} [3, 4] was mistaken for the pacemaker current, even if I_f showed characteristics quite different from those of the pacemaker potential (for example, too negative activation range, activation lag, very slow activation, increasing slope conductance, increasing magnitude and slope in high $[K^+]_o$). By using single Purkinje cells, it was demonstrated that in Tyrode solution the reversal of I_{Kdd} is not spurious, the decrease in slope conductance is not due to K_c depletion but to the decay of I_{Kdd}, the decrease in conductance occurs at potentials positive and negative to E_K, Ba^{2+} blocks the current under study (I_{Kdd}), the unmasked I_f behaves differently from the pacemaker current (more negative range, slow onset, increasing slope conductance, increase with high $[K^+]_o$, etc.). Both I_{Kdd} in Tyrode solution and I_f in the presence of Ba^{2+} are blocked by Cs^+ (non-specific block).

As for the roles of the hyperpolarization-activated current, I_h would protect SAN dominant pacemakers from the hyperpolarizing influence of the more negative atrial muscle cells [29]. On that basis, the elimination of I_h would be expected to cause bradycardia, since dominant pacemakers would no longer be protected from the hyperpolarizing influence of the more negative diastolic potential of surrounding atrial muscle fibers. Other protective actions of I_h might be to counteract the hyperpolarization caused by strong vagal stimulation, to facilitate the subsequent recovery of SAN discharge from vagal inhibition ("postvagal tachycardia", [137]) and to moderate the hyperpolarization induced by fast drive ("overdrive suppression", [138]).

Acknowledgments

The work in author's laboratory was supported by grants from N.I.H. and the American Heart Association, New York Affiliate.

References

1. Vassalle M., Analysis of cardiac pacemaker potential using a "voltage clamp" technique. Am. J. Physiol. 210: 1335–1341, 1966.
2. Vassalle M., Yu H. and Cohen I.S., The pacemaker current in cardiac Purkinje myocytes. J. Gen. Physiol. 106: 559–578, 1995.
3. DiFrancesco D., A new interpretation of the pace-maker current in calf Purkinje fibres. J. Physiol. (Lond.) 314: 359–376, 1981.

4. DiFrancesco D., A study of the ionic nature of the pacemaker current in calf Purkinje fibres. J. Physiol. (Lond.) 314: 377–393, 1981.
5. DiFrancesco D., Funny channels in the control of cardiac rhythm and mode of action of selective blockers. Pharmacol. Res. 53: 399–406, 2006.
6. Noble D., The surprising heart: a review of recent progress in cardiac electrophysiology. J. Physiol. (Lond.) 353: 1–50, 1984.
7. Brown H.F., Electrophysiology of the sinoatrial node. Physiol. Rev. 62: 505–530, 1982.
8. Irisawa H., Brown H.F. and Giles W., Cardiac pacemaking in the sinoatrial node. Physiol. Rev. 73: 197–227, 1993.
9. Vassalle M., Yu H. and Cohen I.S., Pacemaker channels and cardiac automaticity, In: Zipes D.P. and Jalife J. (Eds.), Cardiac Electrophysiology. From Cell to Bedside. WB Saunders Company, Philadelphia, 1999, pp. 94–103.
10. DiFrancesco D., Pacemaker mechanisms in cardiac tissue. Annu. Rev. Physiol. 55: 455–472, 1993.
11. Vassalle M., Mechanisms underlying cardiac pacemaker activity. J. Med. Sci. 23: 249–264, 2003.
12. DiFrancesco D., Serious workings of the funny current. Prog. Biophys. Mol. Biol. 90: 13–25, 2006.
13. Weidmann S., Effect of current flow on the membrane potential of cardiac muscle. J. Physiol. (Lond.) 115: 227–236, 1951.
14. Hutter O.F. and Noble D., Rectifying properties of cardiac muscle. Nature (Lond.) 188: 495, 1960.
15. Hall A.E., Hutter O.F. and Noble D., Current-voltage relations of Purkinje fibres in sodium-deficient solutions. J. Physiol. (Lond.) 166: 225–240, 1963.
16. Vassalle M., Cardiac pacemaker potentials at different extra- and intracellular K concentrations. Am. J. Physiol. 208: 770–775, 1965.
17. Carmeliet E.E., Chloride and potassium permeability in cardiac Purkinje fibres. Arscia S.A. and Presses Académiques Européennes, Bruxelles, 1961.
18. Trautwein W. and Kassebaum D.G., On the mechanism of spontaneous impulse generation in the pacemaker of the heart. J. Gen. Physiol. 45: 317–330, 1961.
19. Noble D. and Tsien R.W., The kinetics and rectifier properties of the slow potassium current in cardiac Purkinje fibres. J. Physiol. (Lond.) 195: 185–214, 1968.
20. Peper K. and Trautwein W., A note on the pacemaker current in Purkinje fibres. Pflügers Arch. 309: 356–361, 1969.
21. Cohen I.S., Daut J. and Noble D., The effects of potassium and temperature on pace-maker current, i_{K2}, in Purkinje fibres. J. Physiol. (Lond.) 260: 55–74, 1976.
22. Seyama I., Characteristics of the rectifying properties of the sino-atrial node cell of the rabbit. J. Physiol. (Lond.) 255: 379–397, 1976.
23. Noma A. and Irisawa H., Membrane currents in the rabbit sinoatrial node cell as studied by the double microelectrode method. Pflügers Arch. 364: 45–52, 1976.
24. Brown H.F., Giles W.R. and Noble S.J., Membrane currents underlying activity in frog sinus venosus. J. Physiol. (Lond.) 271: 783–816, 1977.
25. Seyama I., Characteristics of the anion channel in the sino-atrial node cell of the rabbit. J. Physiol. (Lond.) 294: 447–460, 1979.
26. Brown H.F., DiFrancesco D. and Noble S.J., How does adrenaline accelerate the heart? Nature 280: 235–236, 1979.
27. DiFrancesco D. and Ojeda C., Properties of the current i_f in the sino-atrial node of the rabbit compared with those of the current i_K, in Purkinje fibres. J. Physiol. (Lond.) 308: 353–367, 1980.
28. Noma A., Kotake H. and Irisawa H., Slow inward current and its role mediating the chronotropic effect of epinephrine in the rabbit sinoatrial node. Pflügers Arch. 388: 1–9, 1980.
29. Yanagihara K. and Irisawa H., Inward current activated during hyperpolarization in the rabbit sinoatrial node cell. Pflügers Arch. 385: 11–19, 1980.
30. Yanagihara K. and Irisawa H., Potassium current during the pacemaker depolarization in rabbit sinoatrial node cell. Pflügers Arch. 388: 255–260, 1980.
31. Brown H.F. and DiFrancesco D., Voltage-clamp investigations of membrane currents underlying pace-maker activity in the rabbit sino-atrial node. J. Physiol. (Lond.) 308: 331–351, 1980.
32. Hauswirth O., Noble D. and Tsien R.W., Adrenaline: mechanism of action on the pacemaker potential in cardiac Purkinje fibers. Science 162: 916–917, 1968.
33. McAllister R.E. and Noble D., The time and voltage dependence of the slow outward current in cardiac Purkinje fibres. J. Physiol. (Lond.) 195: 632–662, 1966.
34. Isenberg G., Cardiac Purkinje fibers: cesium as a tool to block inward rectifying potassium currents. Pflügers Arch. 365: 99–106, 1976.
35. Noma A., Morad M. and Irisawa H., Does the "pacemaker current" generate diastolic depolarization in the rabbit SA node cells? Pflügers Arch. 397: 190–194, 1983.
36. Baumgarten C.M. and Isenberg G., Depletion and accumulation of potassium in the extracellular clefts of cardiac Purkinje fibers during voltage clamp hyperpolarization and depolarization. Pflügers Arch. 386: 19–31, 1977.
37. Baumgarten C.M., Isenberg G., McDonald TF and Ten Eick RE, Depletion and accumulation of potassium in the extracellular cleft of cardiac Purkinje fibers during voltage clamp hyperpolarization and depolarization. Experiments in sodium-free bathing media. J. Gen. Physiol. 60: 588–608, 1977.
38. Cohen I.S., Falk R.T. and Mulrine N.K., Actions of barium and rubidium on membrane currents in canine Purkinje fibres. J. Physiol. (Lond.) 338: 589–612, 1983.
39. DiFrancesco D. and Noble D., The influence of voltage non-uniformity on the determination of E_{rev} for i_{K2}. J. Physiol. (Lond.) 297: 158–162, 1979.
40. Draper M.H. and Weidmann S., Cardiac resting and action potentials recorded with an intracellular electrode. J. Physiol. (Lond.) 115: 74–94, 1951.
41. DiFrancesco D. and Noble D., A model of cardiac electrical activity incorporating ionic pumps and concentration changes. Philos. Trans. R. Soc. Lond. (B) 307: 353–398, 1985.
42. Ishikawa S. and Vassalle M., Different forms of spontaneous discharge induced by strophanthidin in cardiac Purkinje fibers. Am. J. Physiol. 243: H767–H778, 1982.
43. Callewaert G., Carmeliet E. and Veerecke J., Single cardiac Purkinje cells: general electrophysiology and voltage-clamp analysis of the pace-maker current. J. Physiol. (Lond.) 349: 643–661, 1984.
44. Sakmann B. and Trube G., Voltage-dependent inactivation of inward-rectifying single-channel currents in the guinea-pig heart cell membrane. J. Physiol. (Lond.) 347: 659–683, 1984.

45. Craven K.B. and Zagotta W.N., CNG and HCN channels: two peas, one pod. Annu. Rev. Physiol. 68: 375–401, 2006.
46. DiFrancesco D. and Tromba C., Muscarinic control of the hyperpolarization-activated current (i_f) in the rabbit sino-atrial myocytes. J. Physiol. (Lond.) 405: 477–491, 1988.
47. Brown H., DiFrancesco D. and Noble S., Cardiac pacemaker oscillation and its modulation by autonomic transmitters. J. Exp. Biol. 81: 175–204, 1979.
48. Yu H., Chang F. and Cohen I.S., Pacemaker current exists in ventricular myocytes. Circ. Res. 72: 232–236, 1993.
49. Zhang H. and Vassalle M., Role of I_K and I_f in the pacemaker mechanisms of sino-atrial node myocytes. Can. J. Physiol. Pharmacol. 79: 963–976, 2001.
50. DiFrancesco D. and Ferroni A., Delayed activation of the cardiac pacemaker current and its dependence on conditioning pre-hyperpolarizations. Pflügers Arch. 396: 265–267, 1983.
51. Sternlicht J.P. and Vassalle M., Cesium, Na^+-K^+ pump and pacemaker potential in cardiac Purkinje fibers. J. Biomed. Sci. 2: 366–378, 1995.
52. Liu Y.M., Yu H., Li C.-Z., Cohen I.S. and Vassalle M., Cs^+ effects on i_f and i_K in rabbit sinoatrial node myocytes: implications for SA node automaticity. J. Cardiovasc. Pharmacol. 32: 783–790, 1998.
53. Sohn H.G. and Vassalle M., Cesium effects on dual pacemaker mechanisms in guinea pig sinoatrial node. J. Mol. Cell. Cardiol. 27: 563–577, 1995.
54. Hauswirth O., Noble D. and Tsien R.W., The mechanism of oscillatory activity at low membrane potentials in cardiac Purkinje fibres. J. Physiol. (Lond.) 200: 255–265, 1969.
55. Vassalle M., Kotake H. and Lin C.-I., Pacemaker current, membrane resistance, and K^+ in sheep cardiac Purkinje fibres. Cardiovasc. Res. 26: 383–391, 1992.
56. Mugelli A., Separation of the oscillatory current from other currents in cardiac Purkinje fibres. Cardiovasc. Res. 16: 637–645, 1982.
57. Nett M.P. and Vassalle M., Obligatory role of diastolic voltage oscillations in sino-atrial node discharge. J. Mol. Cell. Cardiol. 35: 1257–1276, 2003.
58. Kim E.M., Choy Y. and Vassalle M., Mechanisms of suppression and initiation of pacemaker activity in guinea-pig sino-atrial node superfused in high $[K^+]_o$. J. Mol. Cell Cardiol. 29: 1433–1445, 1997.
59. Choy Y., Kim E.M. and Vassalle M., Overdrive excitation in the guinea pig sino-atrial node superfused in high $[K^+]_o$. J. Biomed. Sci. 4: 179–191, 1997.
60. Catanzaro J.N., Nett M.P., Rota M. and Vassalle M., On the mechanisms underlying diastolic voltage oscillations in the sino-atrial node. J. Electrocardiol. 39: 342e1–342e14, 2006.
61. Spiegler P. and Vassalle M., Role of voltage oscillations in the automaticity of sheep cardiac Purkinje fibers. Can. J. Physiol. Pharmacol. 73: 1165–1180, 1995.
62. Noma A., Mechanisms underlying cessation of rabbit sinoatrial node pacemaker activity in high potassium solutions. Jap. J. Physiol. 26: 619–630, 1976.
63. Farès N., Bois P., Lenfant J. and Potreau D., Characterization of a hyperpolarization-activated current in dedifferentiated adult rat ventricular cells in primary culture. J. Physiol. (Lond.) 506: 73–82, 1998.
64. Valenzuela F. and Vassalle M., Role of membrane potential in Ba^{2+}-induced automaticity in guinea pig cardiac myocytes. Cardiovasc. Res. 25: 421–430, 1991.
65. Shen J.-B. and Vassalle M., Cesium abolishes the barium-induced pacemaker potential and current in guinea pig ventricular myocytes. J. Cardiovasc. Electrophysiol. 5: 1031–1044, 1994.
66. Iacono G. and Vassalle M., The interrelationship of cesium, intracellular sodium activity, and pacemaker potential in cardiac Purkinje fibers. Can. J. Physiol. Pharmacol. 68: 1236–1246, 1990.
67. Carmeliet E.E., Decrease in K efflux and influx by external Cs ions in cardiac Purkinje and muscle cells. Pflügers Arch. 383: 143–150, 1980.
68. Eisner D.A. and Lederer W.J., Characterization of the electrogenic sodium pump in cardiac Purkinje fibres. J. Physiol. (Lond.) 303: 441–474, 1980.
69. Vassalle M. and Tamargo J., An analysis of calcium effects on diastolic depolarization in sheep cardiac Purkinje fibers. J. Physiol. (Paris) 85: 27–37, 1991.
70. Chae S.W., Wang D.Y., Gong Q.Y. and Lee C.O., Effect of norepinephrine on Na^+-K^+ pump and Na^+ influx in sheep cardiac Purkinje fibers. Am. J. Physiol. 258: C713–C722, 1990.
71. Glitsch H.G., Pusch H. and Verdonck F., The contribution of Na and K ions to the pacemaker current in sheep cardiac Purkinje fibres. Pflügers Arch. 406: 464–471, 1986.
72. DiFrancesco D., Ferroni A. and Visentin S., Barium-induced blockade of the inward rectifier in calf Purkinje fibres. Pflügers Arch. 402: 446–453, 1984.
73. Cohen I.S. and Falk R.T., The pace-maker current in canine Purkinje fibres. J. Physiol. (Lond.) 308: 30P–31P, 1980 Abstract.
74. Hart G., The kinetics and temperature dependence of the pace-maker current, i_f, in sheep Purkinje fibres. J. Physiol. (Lond.) 337: 401–416, 1983.
75. DiFrancesco D., Characterization of the pace-maker current kinetics in calf Purkinje fibres. J. Physiol. (Lond.) 348: 341–367, 1984.
76. McAllister R.E., Noble D. and Tsien R.W., Reconstruction of the electrical activity of cardiac Purkinje fibres. J. Physiol. (Lond) 251: 1–59, 1975.
77. Brown H.F., Kimura J. and Noble S., The relative contributions of the various time-dependent membrane currents to pacemaker activity in the sino-atrial node, In: Bouman L.N. and Jongsma H.J. (Eds.), Cardiac Rate and Rhythm. Nijhoff, The Hague, 1982, pp. 53–68.
78. Santoro B., Grant S.G., Bartsch D. and Kandel E.R., Interactive cloning with the SH3 domain of N-src identifies a new brain specific ion channel protein, with homology to eag and cyclic nucleotide-gated channels. Proc. Natl. Acad. Sci. U.S.A. 94: 14815–14820, 1997.
79. Pape H.-C., Queer current and the pacemaker: hyperpolarization-activated cation current in neurones. Ann. Rev. Physiol. 58: 299–327, 1996.
80. Santoro B. and Tibbs G.R., The HCN gene family: molecular basis of the hyperpolarization-activated pacemaker channels. Ann N. Y. Acad. Sci. 868: 741–764, 1999.
81. Cohen I.S. and Robinson R.B., Pacemaker current and automatic rhythms: toward a molecular understanding. Handb. Exp. Pharmacol. 171: 41–71, 2005.
82. Zagotta W.N. and Siegelbaum S.A., Structure and function of cyclic nucleotide-gated channels. Annu. Rev. Neurosci. 19: 235–263, 1996.
83. Kaupp U.B. and Seifert R., Cyclic nucleotide-gated ion channels. Physiol. Rev. 82: 769–824, 2002.

84. Biel M., Schneider A. and Wahl C., Cardiac HCN channels: structure, function, and modulation. Trends Cardiovasc. Med. 12: 206–212, 2002.
85. Accili E.A., Proenza C., Baruscotti M. and DiFrancesco D., From funny current to HCN channels: 20 years of excitation. News Physiol. Sci. 17: 32–37, 2003.
86. Matulef K. and Zagotta W.N., Cyclic nucleotide-gated ion channels. Annu. Rev. Cell Dev. Biol. 19: 23–44, 2003.
87. Robinson R.B. and Siegelbaum S.A., Hyperpolarization-activated cation currents: from molecules to physiological function. Annu. Rev. Physiol. 65: 453–480, 2003.
88. Baruscotti M. and DiFrancesco D., Pacemaker channels. Ann. N.Y. Acad. Sci. 1015: 111–121, 2004.
89. Hofmann F., Biel M. and Kaupp U.B., International Union of Pharmacology. LI. Nomenclature and structure-function relationships of cyclic nucleotide-regulated channels. Pharmacol. Rev. 57: 455–462, 2005.
90. Baruscotti M., Bucchi A. and DiFrancesco D., Physiology and pharmacology of the cardiac pacemaker ("funny") current. Pharmacol. Ther. 107: 59–79, 2005.
91. Santoro B., Liu D.T., Yao H., Bartsch D., Kandel E.R., Siegelbaum S.A. and Tibbs G.R., Identification of a gene encoding a hyperpolarizationactivated pacemaker channel of brain. Cell 93: 717–729, 1998.
92. Ludwig A., Zong X., Jeglitsch M., Hofmann F. and Biel M., A family of hyperpolarization-activated mammalian cation channels. Nature 393: 587–591, 1998.
93. Ishii T.M., Takano M., Xie L.-H., Noma A. and Ohmori H., Molecular characterization of the hyperpolarization-activated cation channel in rabbit heart sinoatrial node. J. Biol. Chem. 274: 12835–12839, 1999.
94. Seifert R., Scholten A., Gauss R., Mincheva A., Lichter P. and Kaupp U.B., Molecular characterization of a slowly gating human hyperpolarization-activated channel predominantly expressed in thalamus, heart, and testis. Proc. Natl. Acad. Sci. U.S.A. 96: 9391–9396, 1999.
95. Moosmang S., Stieber J., Zong X., Biel M., Hofmann F. and Ludwig A., Cellular expression and functional characterization of four hyperpolarization-activated pacemaker channels in cardiac and neuronal tissues. Eur. J. Biochem. 268: 1646–1652, 2001.
96. Moosmang S., Biel M., Hofmann F. and Ludwig A., Differential distribution of four hyperpolarization-activated cation channels in mouse brain. Biol. Chem. 380: 975–980, 1999.
97. Santoro B., Chen S., Luthi A., Pavlidis P., Shumyatsky G.P., Tibbs G.R. and Siegelbaum S.A., Molecular and functional heterogeneity of hyperpolarization-activated pacemaker channels in the mouse CNS. J. Neurosci. 20: 5264–5275, 2000.
98. Notomi T. and Shigemoto R., Immunohistochemical localization of Ih channel subunits, HCN1-4, in the rat brain. J. Comp. Neurol. 471: 241–276, 2004.
99. Shi W., Wymore R., Yu H., Wu J., Wymore R.T., Pan Z., Robinson R.B., Dixon J.E., McKinnon D. and Cohen I.S., Distribution and prevalence of hyperpolarization-activated cation channel (HCN) mRNA expression in cardiac tissues. Circ. Res. 85: E1–E6, 1999.
100. Moroni A., Gorza L., Beltrame M., Gravante B., Vaccari T., Bianchi M.E., Altomare C., Longhi R., Heurteaux C., Vitadello M., Malgaroli A. and DiFrancesco D., Hyperpolarization-activated cyclic nucleotide-gated channel is a molecular determinant of the cardiac pacemaker current I_f. J. Biol. Chem. 276: 29233–29241, 2001.
101. Han W., Bao W., Wang Z. and Nattel S., Comparison of ion-channel subunit expression in canine cardiac Purkinje fibers and ventricular muscle. Circ. Res. 91: 790–797, 2002.
102. Zicha S., Fernández-Velasco M., Lonardo G., L'Heureux N. and Nattel S., Sinus node dysfunction and hyperpolarization-activated (HCN) channel subunit remodeling in a canine heart failure model. Cardiovasc. Res. 66: 472–481, 2005.
103. Grafe P., Quasthoff S., Grosskreutz J. and Alzheimer C., Function of the hyperpolarization-activated inward rectification in nonmyelinated peripheral rat and human axons. J. Neurophysiol. 77: 421–426, 1997.
104. Demontis G.C., Longoni B., Barcaro U. and Cervetto L., Properties and functional roles of hyperpolarization-gated currents in guinea-pig retinal rods. J. Physiol. (Lond.) 515: 813–828, 1999.
105. Beaumont V. and Zucker R.S., Enhancement of synaptic transmission by cyclic AMP modulation of presynaptic Ih channels. Nat. Neurosci. 3: 133–141, 2000.
106. Mellor J., Nicoll R.A. and Schmitz D., Mediation of hippocampal mossy fiber long-term potentiation by presynaptic Ih channels. Science 295: 143–147, 2002.
107. Stevens D.R., Seifert R., Bufe B., Muller F., Kremmer E., Gauss R., Meyerhof W., Kaupp U.B. and Lindemann B., Hyperpolarization-activated channels HCN1 and HCN4 mediate responses to sour stimuli. Nature 413: 631–635, 2001.
108. Fain G.L., Quandt FN, Bastian BL, Gerschenfeld HM. Contribution of a caesium-sensitive conductance increase to the rod photoresponse. Nature 272: 466–469, 1978.
109. Altomare C., Terragni B., Brioschi C., Milanesi R., Pagliuca C., Viscomi C., Moroni A., Baruscotti M. and DiFrancesco D., Heteromeric HCN1-HCN4 channels: a comparison with native pacemaker channels from the rabbit sinoatrial node. J. Physiol. (Lond.) 549: 347–359, 2003.
110. Ludwig A., Zong X., Stieber J., Hullin R., Hofmann F. and Biel M., Two pacemaker channels from human heart with profoundly different activation kinetics. EMBO J. 18: 2323–2329, 1999.
111. Kaupp U.B. and Seifert R., Molecular diversity of pacemaker ion channels. Annu. Rev. Physiol. 63: 235–257, 2001.
112. Altomare C., Bucchi A., Camatini E., Baruscotti M., Viscomi C., Moroni A. and DiFrancesco D., Integrated allosteric model of voltage gating of HCN channels. J. Gen. Physiol. 117: 519–532, 2001.
113. DiFrancesco D. and Tortora P., Direct activation of cardiac pacemaker channelsby intracellular cyclic AMP. Nature 351: 145–147, 1991.
114. DiFrancesco D. and Mangoni M., Modulation of single hyperpolarization-activated channels (i(f)) by cAMP in the rabbit sino-atrial node. J. Physiol. 474: 473–482, 1994.
115. Bois P., Renaudon B., Baruscotti M., Lenfant J. and DiFrancesco D., Activation of f-channels by cAMP analogues in macropatches from rabbit sino-atrial node myocytes. J. Physiol. (Lond.) 501: 565–571, 1997.
116. Baker K., Warren K.S., Yellen G. and Fishman M.C., Defective 'pacemaker' current (Ih) in a zebrafish mutant with a slow heart rate. Proc. Natl. Acad. Sci. U.S.A. 94: 4554–4559, 1997.
117. Cerbai E., Barbieri M. and Mugelli A., Occurrence and properties of the hyperpolarization-activated current If in

ventricular myocytes from normotensive and hypertensive rats during aging. Circulation 94: 1674–1681, 1996.
118. Hoppe U.C., Jansen E., Südkamp M. and Beuckelmann D.J., Hyperpolarization-activated inward current in ventricular myocytes from normal and failing human hearts. Circulation 97: 55–65, 1998.
119. Vaccari T., Moroni A., Rocchi M., Gorza L., Bianchi M.E., Beltrame M. and DiFrancesco D., The human gene coding for HCN2, a pacemaker channel of the heart. Biochim. Biophys. Acta. 1446: 419–425, 1999.
120. Qu J., Plotnikov A.N., Danilo Jr. P., Shlapakova I., Cohen I.S., Robinson R.B. and Rosen M.R., Expression and function of a biological pacemaker in canine heart. Circulation 107: 1106–1109, 2003.
121. Wang J., Chen S. and Siegelbaum S.A., Regulation of hyperpolarization-activated HCN channel gating and cAMP modulation due to interactions of COOH terminus and core transmembrane regions. J. Gen. Physiol. 118: 237–250, 2001.
122. Craven K.B. and Zagotta W.N., Salt bridges and gating in the COOH-terminal region of HCN2 and CNGA1 channels. J. Gen. Physiol. 124: 663–677, 2004.
123. Zhou L., Olivier N.B., Yao H., Young E.C. and Siegelbaum S.A., A conserved tripeptide in CNG and HCN channels regulates ligand gating by controlling C-terminal oligomerization. Neuron 2004 44: 823–834, 2004.
124. BoSmith R.E., Briggs I. and Sturgess N.C., Inhibitory actions of ZENECA ZD7288 on whole-cell hyperpolarization activated inward current (I_f) in guinea-pig dissociated sinoatrial node cells. Br. J. Pharmacol. 110: 343–349, 1993.
125. Doerr T. and Trautwein W., On the mechanism of the "specific bradycardic action" of the verapamil derivative UL-FS 49. Naunyn-Schmiedebergs Arch Pharmacol 341: 331–340, 1990.
126. Valenzuela C., Delpon E., Franqueza L., Gay P., Perez O., Tamargo J. and Snyders D.J., Class III antiarrhythmic effects of zatebradine. Time-, state-, use-, and voltage-dependent block of hKv1.5 channels. Circulation 94: 562–570, 1996.
127. Chen C., ZD7288 inhibits postsynaptic glutamate receptor-mediated responses at hippocampal perforant path-granule cell synapses. Eur. J. Neurosci. 19: 643–649, 2004.
128. Bucchi A., Baruscotti M. and DiFrancesco D., Current-dependent block of rabbit sino-atrial node I_f channels by ivabradine. J. Gen. Physiol. 120: 1–13, 2002.
129. Stieber J., Herrmann S., Feil S., Loster J., Feil R., Biel M., Hofmann F. and Ludwig A., The hyperpolarization-activated channel HCN4 is required for the generation of pacemaker action potentials in the embryonic heart. Proc. Natl. Acad. Sci. U.S.A. 100: 15235–15240, 2003.
130. Lei M., Goddard C., Liu J., Leoni A.L., Royer A., Fung S.S., Xiao G., Ma A., Zhang H., Charpentier F., Vandenberg J.I., Colledge W.H., Grace A.A. and Huang C.L., Sinus node dysfunction following targeted disruption of the murine cardiac sodium channel gene Scn5a. J. Physiol. 567: 387–400, 2005.
131. Platzer J., Engel J., Schrott-Fischer A., Stephan K., Bova S., Chen H., Zheng H. and Striessnig J., Congenital deafness and sinoatrial node dysfunction in mice lacking class D L-type Ca2+ channels. Cell 102: 89–97, 2000.
132. Zhang Z., Xu Y., Song H., Rodriguez J., Tuteja D., Namkung Y., Shin H.S. and Chiamvimonvat N., Functional Roles of Ca(v)1.3 (alpha(1D)) calcium channel in sinoatrial nodes: insight gained using gene-targeted null mutant mice. Circ. Res. 90: 981–987, 2002.
133. Mangoni M.E., Traboulsie A., Leoni A.L., Couette B., Marger L., Le Quang K., Kupfer E., Cohen-Solal A., Vilar J., Shin H.S., Escande D., Charpentier F., Nargeot J. and Lory P., Bradycardia and slowing of the atrioventricular conduction in mice lacking CaV3.1/alpha1G T-type calcium channels. Circ. Res. 98: 1422–1430, 2006.
134. Earm Y.E., Shimoni Y. and Spindler A.J., A pace-maker-like current in the sheep atrium and its modulation by catecholamines. J. Physiol. (London) 342: 569–590, 1983.
135. Porciatti F., Pelzmann B., Cerbai E., Schaffer P., Pino R., Bernhart E., Koidl B. and Mugelli A., The pacemaker current I(f) in single human atrial myocytes and the effect of beta-adrenoceptor and A1-adenosine receptor stimulation. Br. J. Pharmacol. 122: 963–969, 1997.
136. Zhang H. and Vassalle M., On the mechanisms of adrenergic control of the sino-atrial node discharge. J. Biomed. Sci. 10: 179–192, 2003.
137. Copen D.L., Cirillo D.P. and Vassalle M., Tachycardia following vagal stimulation. Am. J. Physiol. 215: 696–703, 1968.
138. Vassalle M., Electrogenic suppression of automaticity in sheep and dog Purkinje fibers. Circ. Res. 27: 361–377, 1970.